LINEAR POLARIZATION OBSERVATIONS OF GALACTIC RADIO EMISSION AT 620 AND 408 Mc/s

By D. S. Mathewson,* N. W. Broten,* and D. J. Cole*

[*Manuscript received September* 9, 1965]

Summary

Observations at 620 and 408 Mc/s have been used to determine the intrinsic polarization of galactic radio emission in the strong extended regions of the band of polarization discovered at 408 Mc/s. Many of the intrinsic polarization angles lie nearly parallel to the approximate midline of the band, i.e. the great circle passing through the galactic poles and intersecting the plane at $l^{\mathrm{II}} = 340°$ and 160°. This new observational evidence supports the explanation proposed by Mathewson and Milne in 1965 for the existence of the band, namely, that the emission is synchrotron radiation from regions in the local spiral arm that are pervaded by a fairly uniform magnetic field parallel to the galactic plane and directed towards $l^{\mathrm{II}} = 70°$ or 250°.

I. Introduction

Mathewson and Milne (1965, hereafter referred to as Paper I) have shown that almost all of the polarized galactic radio emission at 408 Mc/s lies in a band about 60° wide that contains the great circle passing through the galactic poles and intersecting the plane at $l^{\mathrm{II}} = 340°$ and 160°. The explanation proposed in Paper I for this particular distribution of polarization was that the emission is synchrotron radiation from regions in the local spiral arm that are pervaded by a fairly uniform magnetic field parallel to the line joining $b^{\mathrm{II}} = 0°$, $l^{\mathrm{II}} = 70°$ and $b^{\mathrm{II}} = 0°$, $l^{\mathrm{II}} = 250°$. If this is correct, the intrinsic direction of the E vectors of the radiation, which are perpendicular to the magnetic field at emission, should be approximately parallel to this great circle.

To test this, linear polarization observations at 620 Mc/s were made at 195 positions in the strong extended regions of polarization found at 408 Mc/s (Paper I). The 408 Mc/s polarization measurements were also repeated at these positions. The intrinsic polarization angles were calculated from the observations at these two frequencies, and the results are discussed in Section V.

In addition, linear polarization was looked for, and detected at 37 of the positions, at the higher frequency of 1410 Mc/s. The results of these observations are given in Table 4 (Section IV).

II. Equipment

The observations were made with the CSIRO 210 ft radio telescope at Parkes, N.S.W. At each frequency of observation, the reflector was fed by a pair of parallel dipoles with a plane reflector, giving a tapered illumination which fell to approxi-

* Division of Radiophysics, CSIRO, University Grounds, Chippendale, N.S.W.

mately 4% at the edge of the aperture. To change the polarization, the aerial feed could be rotated at 3°/sec through one complete revolution in either direction.

The aerial beamwidths and receiver parameters at the three frequencies used in the observations are given in Table 1. A 2 sec time constant was used at each frequency.

The sensitivity of the system was calibrated using the radio source Hydra A. The flux densities of Hydra A at the three frequencies were taken from Kellermann

TABLE 1

AERIAL BEAMWIDTHS AND RECEIVER PARAMETERS

Frequency (Mc/s)	Aerial Beamwidth (min arc)	Receiver Bandwidth (Mc/s)	Peak-to-peak Noise (degK)
1410	14	10	0·15
620	32	double-sideband, each 8 Mc/s	0·5
408	48	double-sideband, each 8 Mc/s	0·5

TABLE 2

CALIBRATION POINTS FOR THE THREE FREQUENCIES OF OBSERVATION

Frequency (Mc/s)	Position (1964)		θ_{eq} (outside-ionosphere)	T_b^p (°K)
	R.A. (hr)	Dec. (deg)		
408	1400	−20	135	4·5
	1840	−14	154	7·0
	1924	−52	65	4·0
	2048	−36	87	5·2
	0216	+12	9	5·4
520	1456	−10	134	4·6
	1840	−14	20	2·4
	1924	−52	86	2·4
	2036	−40	77	2·5
	0216	+12	169	2·9
1410	1440	−14	132	0·7
	1912	−44	136	0·6
	2000	−56	66	0·6

(1964). Following Seeger, Westerhout, and van de Hulst (1956), measurements of the aerial polar diagrams at the three frequencies were used to show that a point source of $1\cdot 14\times 10^{-26}$ W m^{-2} (c/s)$^{-1}$ at the centre of the aerial beam would increase the full-beam brightness temperature T_b by 1 degK. By use of this relationship, deflections on the chart recorder, when measured in fractions of the deflection obtained from Hydra A, were converted into units of brightness temperature.

III. Observational Procedure and Data Reduction

The observational procedure and data reduction process used in the present survey were the same as those described in Section III of Paper I.

The observations, which were carried out during the latter half of 1964, were made at night to avoid effects of solar radiation and rapid changes in the ionosphere. The observational procedure was to track the position whilst rotating the feed through about 300° in each direction. The 408 Mc/s observations were made during the first few nights of an observing period. On the following nights, the same positions were observed at 620 Mc/s, and on the final nights some of the positions were observed at 1410 Mc/s.

The instrumental polarized component was determined using the unpolarized positions given in Paper I plus a position at R.A. $05^{\mathrm{h}}36^{\mathrm{m}}$, Dec. −30° which was used for the 1410 Mc/s observations. Table 2 lists a number of strongly polarized positions at each frequency of observation, which were used for checking the overall system. The "outside-ionosphere" position angle of the E vector, θ_{eq}, and the polarization brightness temperature $T_{\mathrm{b}}^{\mathrm{p}}$ are given for each position.

Correction was made for the Faraday rotation in the ionosphere using the same method as described in Section III of Paper I. The sense of rotation was such that, for all points in the survey, the observed values of the polarization angles were less than the values outside the ionosphere. The corrections at 620 Mc/s were all less than 10°. No corrections were made to the 1410 Mc/s observations for ionospheric Faraday rotation.

IV. Presentation of Results

The results of the polarization measurements at 620 and 408 Mc/s are given in three forms: (*a*) tabular presentation; (*b*) E-vector presentation; (*c*) rotation measures and spectral index diagram.

(*a*) *Tabular Presentation*

The results of the observations at 620 and 408 Mc/s are set out in Table 3, the explanation of which is given below.

Columns 1 and 2.—Right ascensions and declinations (epoch 1964) at which the measurements were made. An asterisk against the right ascension indicates that observations were also made at 1410 Mc/s (see Table 4). A dagger indicates that the polarization at this position was measured at 440 Mc/s (see part (*c*) of this section).

Columns 3 and 4.—θ_{eq}, the position angle at 620 and 408 Mc/s of the plane of vibration of the incident E vector, measured from the celestial north pole in the direction of increasing right ascension (east). This value is not corrected for ionospheric Faraday rotation. The probable error in the measurement of θ_{eq} is about 5° at both frequencies.

Columns 5 and 6.—$T_{\mathrm{b}}^{\mathrm{p}}$, the polarization brightness temperature at 620 and 408 Mc/s. The probable error of the 620 and 408 Mc/s measurements is about 0·4 degK. At 620 Mc/s, polarization temperatures less than 0·8°K have not been given as it was felt that at this low level of $T_{\mathrm{b}}^{\mathrm{p}}$ the results were not significant.

TABLE 3

RESULTS OF LINEAR POLARIZATION OBSERVATIONS AT 620 AND 408 MC/S

Position (1964) R.A. (hr)	Position (1964) Dec. (deg)	θ_{eq} (inside-ionosphere) 620	θ_{eq} (inside-ionosphere) 408	T_b^p (°K) 620	T_b^p (°K) 408	θ_{gal} (outside-ionosphere) 620	θ_{gal} (outside-ionosphere) 408	l^{II} (degrees)	b^{II} (degrees)
1330	0	168	22	1·5	5·2	16	62	324	+61
1340	0	177	18	2·1	4·8	30	63	329	+60
*1350	+8	144	137	2·6	3·8	7	12	342	+66
1350	+12	178	47	2·8	4·1	49	109	349	+69
1350	+14	155	12	4·0	4·8	27	76	353	+70
1350	+16	155	168	4·7	4·6	32	57	357	+72
*†1400	+8	163	8	3·8	5·0	31	68	347	+64
*†1400	+10	167	7	3·6	6·7	37	69	350	+66
*†1400	+12	165	21	3·8	7·2	39	87	354	+67
1400	−16	131	127	1·0	3·4	162	169	327	+43
1400	−18	128	110	1·5	3·7	158	152	326	+41
1400	−20	130	120	1·5	4·5	159	161	325	+40
1408	−14	134	122	1·5	2·9	167	167	330	+44
1408	−16	130	111	1·0	3·5	163	156	329	+43
1410	−18	129	119	1·5	4·2	161	163	329	+41
1410	−20	136	145	1·3	3·5	168	9	328	+39
*1416	−12	133	95	2·8	3·4	170	144	334	+45
1416	−16	130	119	1·5	4·1	166	167	332	+42
*1420	−18	133	126	1·9	4·0	169	174	331	+40
1420	−20	126	157	1·0	2·9	161	24	330	+38
1424	−14	123	117	1·6	4·2	162	168	335	+43
1424	−16	129	121	1·2	3·0	166	170	334	+41
*1430	−18	139	130	1·9	3·0	176	179	334	+38
*†1432	−14	146	122	2·5	4·1	7	175	337	+42
*1432	−16	127	123	2·3	3·0	168	174	336	+40
1440	−10	120	96	1·7	3·1	165	153	343	+44
*†1440	−12	142	114	3·0	5·0	6	170	341	+42
*†1440	−14	133	100	3·3	4·2	175	154	340	+41
*†1448	−10	124	112	3·2	4·7	170	170	345	+43
*1448	−12	165	134	2·4	3·3	30	11	343	+41
*1456	−6	127	108	1·8	3·7	177	170	350	+45
*1456	−8	116	100	3·0	4·7	165	161	349	+43
*1456	−10	125	99	4·6	3·3	173	159	347	+42
*†1504	−8	149	40	3·2	5·4	19	22	351	+42
1512	−6	171	113	1·2	3·7	45	179	354	+42
1516	−5	170	83	1·7	2·6	45	150	356	+42
1546	−56	110	117	2·4	3·8	151	165	326	−2
*†1602	−56	110	110	1·3	3·1	154	158	328	−3
*†1602	−58	112	115	1·0	2·5	156	163	326	−4
*†1618	−58	115	109	1·0	2·6	163	161	328	−6
*1634	−60	105	125	1·0	2·8	156	0	328	−9
1650	−56	—	102	$<0·8$	2·8	—	161	332	−8
1700	−48	120	106	1·5	2·3	176	166	340	−4
1712	−48	113	86	1·3	2·3	172	150	341	−6
*†1840	−14	12	137	2·4	7·0	82	35	20	−4
*†1840	−16	42	162	1·9	5·2	111	60	18	−5
*1848	−16	36	141	1·3	3·9	104	39	19	−7
*1848	−18	33	137	1·6	3·6	103	36	17	−8

TABLE 3 (*Continued*)

Position (1964) R.A. (hr)	Position (1964) Dec. (deg)	θ_{eq} (inside-ionosphere) 620	θ_{eq} (inside-ionosphere) 408	T_b^p (°K) 620	T_b^p (°K) 408	θ_{gal} (outside-ionosphere) 620	θ_{gal} (outside-ionosphere) 408	l^{II} (degrees)	b^{II} (degrees)
*1848	−20	37	143	1·9	4·0	107	42	15	−9
*1858	−64	—	63	<0·8	2·6	—	148	332	−25
1900	−46	97	83	1·4	3·5	175	172	351	−21
*1900	−48	66	61	2·3	3·6	145	150	349	−22
1900	−50	92	65	1·5	3·7	171	154	347	−22
1900	−52	75	68	1·3	4·2	155	158	345	−23
*1900	−54	97	79	2·1	3·0	176	170	343	−23
1900	−56	99	80	1·4	3·0	1	172	341	−24
1900	−66	85	63	1·1	2·6	168	150	330	−26
*1912	−38	79	39	1·9	3·0	155	125	0	−21
1912	−42	90	47	1·7	3·7	169	136	356	−22
*†1912	−44	100	99	2·0	3·0	179	6	354	−23
†1912	−48	92	50	1·5	4·3	173	141	350	−24
1912	−50	83	55	1·2	4·3	164	146	348	−24
1912	−52	67	60	1·0	3·5	149	152	345	−25
1912	−54	99	69	1·2	3·5	2	162	343	−25
1912	−56	91	72	1·3	2·9	175	166	341	−26
1915	−58	97	70	1·6	2·8	3	166	339	−26
*1915	−60	100	78	1·4	3·1	4	166	337	−27
*1915	−64	94	70	1·0	2·5	0	160	332	−27
1915	−66	60	74	1·1	2·8	148	165	330	−28
1915	−68	80	95	1·0	3·1	168	7	328	−28
*1924	−36	75	51	1·8	3·5	152	137	3	−22
1924	−38	75	24	1·3	3·0	153	112	1	−23
1924	−40	68	29	1·5	3·2	147	118	359	−24
†1924	−42	92	44	1·5	3·7	172	134	357	−24
1924	−44	67	43	1·3	3·7	148	134	354	−25
1924	−46	100	56	1·0	3·8	2	148	352	−25
*1924	−48	83	47	2·0	3·0	165	139	350	−26
1924	−50	82	50	1·5	3·2	166	144	348	−26
*1924	−52	80	49	2·4	4·0	164	143	346	−26
†1924	−54	68	58	1·7	3·7	154	154	344	−27
*†1924	−56	78	82	2·4	4·5	164	178	341	−27
*1930	−58	101	82	1·9	4·0	9	0	339	−28
*1930	−60	70	70	2·2	2·8	157	161	337	−29
*1930	−62	58	47	1·8	3·3	145	138	335	−29
*1930	−64	60	42	1·2	2·8	148	134	333	−29
*1930	−68	—	72	<0·8	3·5	—	167	328	−29
1936	−42	87	51	1·3	2·8	169	143	357	−26
*1936	−50	44	20	2·0	2·9	130	116	348	−28
1936	−52	64	27	1·2	4·3	151	124	346	−28
*1936	−54	50	41	2·2	4·3	138	139	344	−29
1936	−56	87	72	1·4	3·0	176	171	342	−29
1945	−58	89	65	1·0	3·3	0	166	340	−30
*1945	−66	97	70	1·1	3·1	11	168	330	−30
*1945	−68	70	50	1·0	4·5	164	148	328	−30
*1948	−52	57	0	2·5	3·2	146	99	347	−30
*†1948	−54	67	20	2·1	2·8	157	120	344	−30

* Observations also made at 1410 Mc/s (see Table 4).

† Polarization at this position measured at 440 Mc/s.

TABLE 3 (*Continued*)

Position (1964) R.A. (hr)	Dec. (deg)	θ_{eq} (inside-ionosphere) 620	408	T_b^p (°K) 620	408	θ_{gal} (outside-ionosphere) 620	408	l^{II} (degrees)	b^{II}
†1948	−56	79	58	1·7	4·1	170	159	342	−31
*2000	−54	62	29	2·3	4·0	154	131	344	−32
*2000	−56	75	58	2·0	4·7	169	162	342	−32
2000	−58	80	62	1·2	4·0	174	166	340	−32
2000	−60	88	76	1·7	2·8	0	173	337	−32
2012	−46	74	47	2·5	3·0	161	138	354	−33
2012	−48	—	27	<0·8	3·4	—	119	352	−34
2012	−56	68	31	1·6	3·3	164	137	342	−34
*2015	−70	54	0	1·8	3·1	157	107	325	−33
*2015	−72	39	32	1·8	4·3	144	141	323	−33
2024	−40	—	61	<0·8	3·1	—	152	2	−35
2024	−46	59	57	2·1	2·6	148	150	354	−35
2024	−48	38	23	1·7	2·8	128	117	352	−36
2024	−54	33	153	1·5	3·4	127	71	344	−36
*2030	−70	89	9	1·0	3·7	15	119	325	−34
2036	−40	72	92	2·5	2·6	160	6	2	−37
2036	−42	69	50	1·5	3·0	157	144	359	−37
2036	−52	45	8	1·3	2·6	141	108	347	−37
2036	−54	36	174	2·0	2·9	136	96	344	−37
2048	−36	50	74	1·0	5·2	138	170	7	−39
†2048	−38	55	99	1·3	3·7	145	17	5	−39
*†2048	−40	91	116	2·0	4·3	3	36	2	−39
†2048	−42	178	89	1·0	5·5	91	10	0	−39
*2048	−44	72	71	1·8	4·3	167	174	357	−40
*2055	−72	16	19	1·4	3·4	131	138	322	−36
2100	−44	61	64	1·0	4·8	158	169	357	−42
*2100	−46	81	81	2·0	4·4	179	7	354	−42
*2100	−48	44	54	1·9	4·1	145	163	352	−42
*†2100	−50	77	50	2·0	3·9	179	160	349	−41
*†2100	−52	61	67	2·3	4·3	168	2	346	−41
2112	−34	71	65	1·9	4·1	161	163	11	−43
*2112	−36	72	80	2·0	4·0	163	179	8	−44
2112	−46	25	112	1·4	2·5	122	35	354	−44
*2112	−48	28	50	2·0	4·4	131	161	352	−44
*†2112	−50	46	52	2·5	4·8	150	164	349	−43
2112	−52	31	42	1·4	4·5	137	156	346	−43
*2120	−72	171	3	1·1	4·8	112	128	321	−37
2124	−32	58	43	1·4	4·5	147	140	14	−46
*2124	−34	68	77	2·3	4·2	159	176	11	−46
2124	−40	65	12	1·0	3·2	160	112	3	−46
2124	−42	77	41	1·0	3·0	173	143	0	−46
2124	−44	75	25	1·9	2·7	173	129	357	−46
*2124	−48	50	73	1·9	3·5	155	6	351	−46
*†2124	−50	60	58	2·7	4·3	167	173	348	−45
†2124	−52	38	53	1·3	5·5	147	170	346	−45
2124	−54	51	52	1·3	4·1	162	171	343	−44
*2124	−56	35	81	1·0	3·3	144	13	340	−44
*2136	−40	75	28	1·8	3·0	174	135	3	−48
†2136	−42	110	72	1·5	5·0	31	1	0	−48
*†2136	−44	94	26	2·3	4·4	16	137	357	−48

TABLE 3 (*Continued*)

Position (1964) R.A. (hr)	Position (1964) Dec. (deg)	θ_{eq} (inside-ionosphere) 620	θ_{eq} (inside-ionosphere) 408	T_b^p (°K) 620	T_b^p (°K) 408	θ_{gal} (outside-ionosphere) 620	θ_{gal} (outside-ionosphere) 408	l^{II} (degrees)	b^{II} (degrees)
2136	−46	90	72	1·0	3·7	16	6	354	−48
2136	−48	11	55	2·2	3·0	116	164	351	−48
2136	−50	57	73	1·4	3·8	167	11	348	−47
†2136	−52	56	111	1·3	3·0	168	51	345	−47
2136	−54	40	53	1·2	4·6	154	175	342	−46
*2145	−58	—	104	<0·8	3·4	—	44	336	−46
*2145	−60	—	88	<0·8	3·8	—	30	334	−45
2145	−70	35	30	1·3	2·7	162	161	322	−40
*2145	−72	9	44	1·0	3·5	136	175	320	−39
*2148	−44	123	94	2·0	5·0	49	28	356	−50
2148	−46	124	84	1·3	3·9	51	20	353	−50
2148	−50	27	52	2·2	3·1	137	166	347	−49
*2148	−56	—	86	<0·8	3·2	—	26	339	−47
2200	−46	156	135	1·0	3·3	87	74	352	−52
*2200	−56	83	78	1·7	3·0	22	21	338	−49
*2200	−66	41	26	1·6	2·8	168	157	325	−43
*2215	−66	66	61	1·0	3·8	18	17	324	−45
*2215	−70	177	28	1·0	3·6	132	167	320	−42
*2230	−64	104	127	1·0	2·9	58	85	325	−47
*2230	−66	45	104	1·1	2·4	0	63	322	−46
*0118	+8	144	134	1·8	5·3	145	146	135	−54
0122	+2	160	146	1·4	5·8	155	153	139	−60
0126	+6	138	123	1·5	5·0	133	130	139	−55
†0126	+8	156	117	1·5	7·0	151	124	139	−53
0126	+10	118	105	1·2	5·2	117	116	138	−52
*0132	+6	161	5	2·2	5·3	155	11	142	−55
*†0132	+8	135	124	2·2	6·5	129	130	141	−53
*†0132	+10	123	106	2·1	6·0	117	112	140	−51
*0140	+6	8	44	2·0	5·2	178	46	145	−54
*0148	+6	179	51	2·0	4·4	169	50	148	−54
*0148	+8	14	42	1·9	7·0	2	42	147	−52
0156	+6	174	16	1·2	4·4	158	12	151	−53
0156	+8	178	14	1·6	4·8	164	12	150	−51
*0156	+10	162	10	2·0	6·3	149	9	149	−49
*0200	+8	160	8	1·8	7·7	144	4	151	−51
*†0200	+10	161	179	1·8	6·8	147	177	150	−49
*0200	+12	149	178	1·8	5·4	136	177	149	−47
*0208	+8	177	18	2·3	6·6	159	12	154	−50
0208	+10	153	177	1·6	8·5	136	172	153	−48
0208	+12	144	171	1·7	6·2	128	167	152	−46
0216	+8	4	23	2·0	5·9	164	15	157	−49
*†0216	+10	160	5	2·3	6·3	141	178	155	−47
*†0216	+12	159	167	2·9	5·4	141	161	154	−45
0224	+8	15	77	1·5	4·3	172	66	159	−48
0224	+10	23	73	2·2	5·4	3	65	158	−46
0224	+12	170	44	1·3	5·4	151	37	156	−44
0232	+8	24	120	1·8	4·5	0	108	162	−47
0232	+14	168	19	2·4	4·8	146	9	157	−42

* Observations also made at 1410 Mc/s (see Table 4).

† Polarization at this position measured at 440 Mc/s.

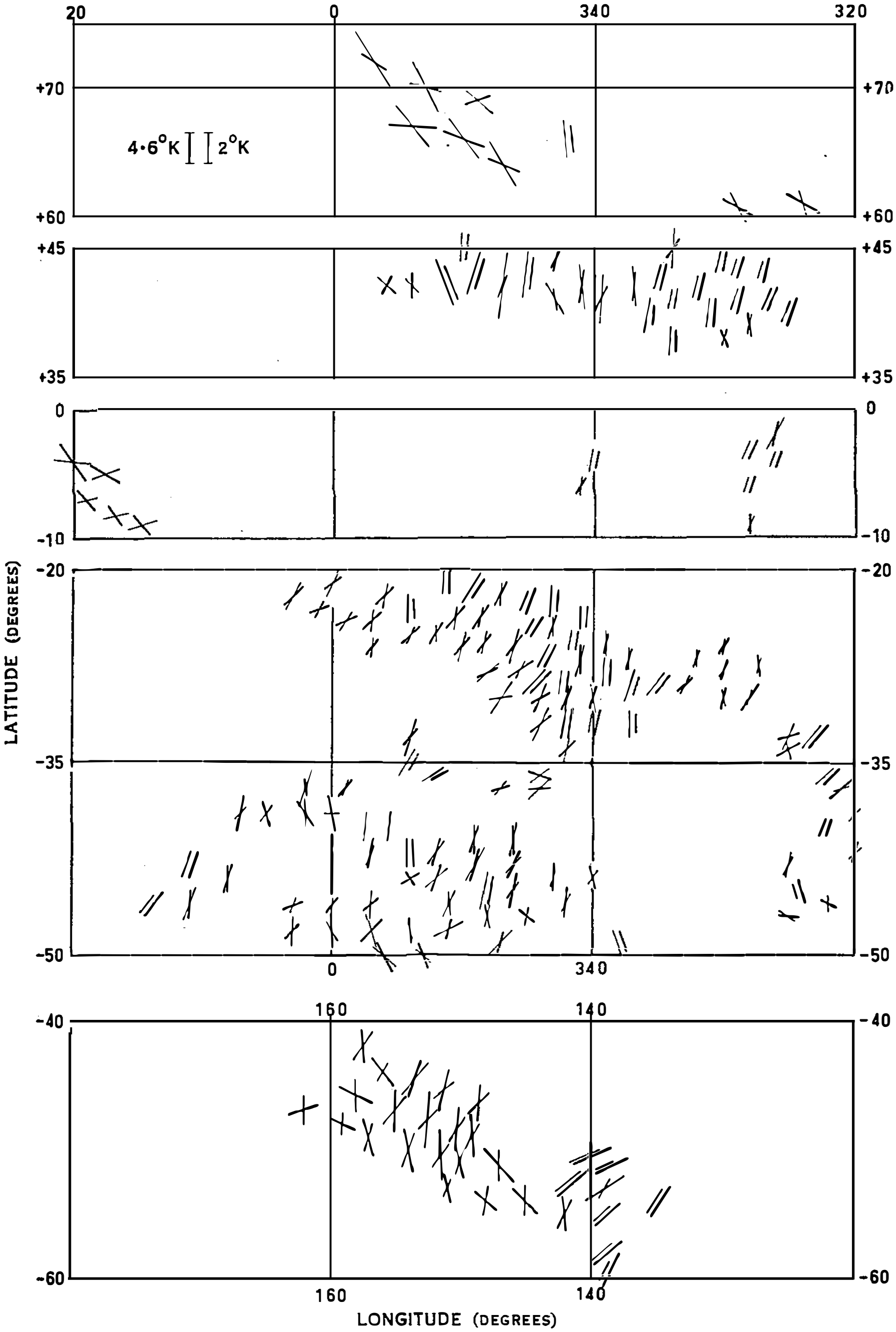

Fig. 1.—The 620 Mc/s (——) and 408 Mc/s (——) E vectors plotted as lines centred on the positions (new galactic coordinates) of the observed points. The angle at which each line is drawn relative to the direction of the galactic north pole, in the direction of increasing longitude, is θ_{gal}, and the length of each line is proportional to the polarization brightness temperature (see scale at top). The 620 Mc/s temperature scale is $2 \cdot 3$ (the square of the frequency ratio) times the 408 Mc/s scale.

Columns 7 and 8.—θ_{gal}, the galactic position angle at 620 and 408 Mc/s of the plane of vibration of the incident E vector, measured from the galactic north pole in the direction of increasing longitude. This is obtained by adding to θ_{eq} the galactic parallactic angle and the correction for Faraday rotation in the ionosphere.

Columns 9 and 10.—Galactic longitude l^{II} and galactic latitude b^{II} (to the nearest degree) of the position of observation.

(b) E-*vector Presentation*

In Figure 1, the 620 and 408 Mc/s E vectors are plotted as lines centred on the positions of the observed points. When the angle between the 620 Mc/s (light line) and 408 Mc/s (heavy line) E vectors is very small, the lines are separated and the observed position lies at the midpoint between the lines.

The angle at which each line is drawn relative to the galactic north pole in the direction of increasing longitude is θ_{gal} (corrected for ionospheric Faraday rotation), and the length of each line is proportional to $T_{\mathrm{b}}^{\mathrm{p}}$. The scale of the polarization temperature at 620 Mc/s is $2 \cdot 3$ (the square of the frequency ratio) times the 408 Mc/s temperature scale. When the angular structure of the polarized radiation is large compared with the 408 Mc/s beamwidth, equality of the lengths at the two frequencies corresponds to an apparent flux-density spectral index of 0 for the polarized radiation.

(c) *Rotation Measure and Spectral Index Diagram*

It has been found by Cooper and Price (1962) and Gardner and Whiteoak (1963) that for radio sources the position angle of the E vector of the polarized component varies as the square of the wavelength. This result is consistent with Faraday rotation in an ionized gas. The relationship can be expressed (Gardner and Whiteoak 1963) as

$$\theta = \theta_{\mathrm{intr}} + (\mathrm{R.M.})\lambda^2,$$

where θ_{intr} is the intrinsic polarization angle, i.e. the direction of the E vector at emission. For synchrotron radiation, θ_{intr} is perpendicular to the projection of the magnetic field on the sky. R.M., the rotation measure, measures the integrated value of the longitudinal-field–electron-density product along the line-of-sight. Numerically, with R.M. expressed in radians/metre^2,

$$\mathrm{R.M.} = 8 \cdot 1 \times 10^5 \int N B_{\mathrm{L}} \, \mathrm{d}L,$$

where the electron density N is in electrons/cm^3, the longitudinal magnetic field B_{L} is in gauss, and the path length L is in parsecs.

Between the frequencies 620 and 408 Mc/s there is an ambiguity in the angle through which the E vector rotates. To remove this ambiguity, some observations were made at 440 Mc/s at the positions indicated by daggers in Table 3. It was found that θ_{eq} at 440 Mc/s was always within 10° of θ_{eq} at 408 Mc/s. Consequently, it is assumed that the angle of rotation between 620 and 408 Mc/s is the minimum possible. The rotation measure is calculated on this basis and in Figure 2 is given

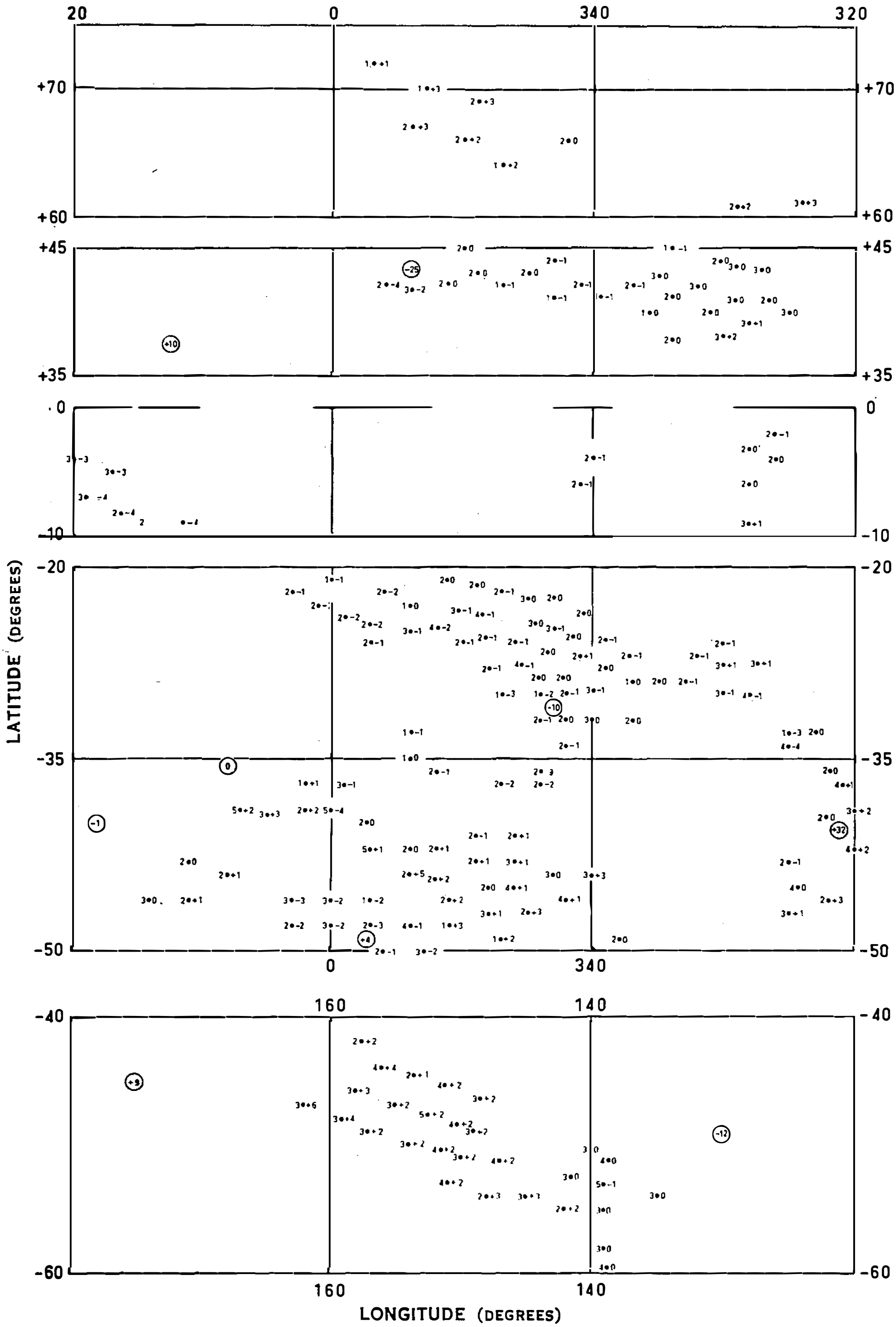
20
0
340
320
+70
+60
+45
+35
0
-10
-20
-35
-50
340
160
140
-40
-60
LATITUDE (DEGREES)
LONGITUDE (DEGREES)

Fig. 2

(to the nearest integer) by the number to the right of the dot that indicates the position of measurement. A rotation measure of 1 corresponds to a difference of 18° between the polarization angles at 620 and 408 Mc/s. The rotation measure is positive if the magnetic field is directed towards the observer.

The number to the left of the position dot (Fig. 2) is the ratio of the polarization temperatures at 408 and 620 Mc/s, to the nearest integer. This number gives a measure of the apparent spectral index of the polarized radiation. A ratio of 2 would indicate that the flux-density spectral index is approximately zero, whilst a ratio of 3 would indicate a spectral index of $-0\cdot6$, which is the value found for unpolarized galactic radio emission (Wielebinski and Yates 1965).

Polarization measurements at 1410 Mc/s were made at 95 of the positions given in Table 3. They have been marked with asterisks. Table 4 gives the positions at which polarization was successfully detected ($T_b^p > 0\cdot3$°K) together with their polarization angles and temperatures. The intrinsic polarization angles of these points are given for comparison in the last column. They were derived from the rotation measures calculated from the 620 and 408 Mc/s results.

V. Discussion of Results

(a) *Intrinsic Polarization Angles*

The main purpose of the present project was to calculate the intrinsic polarization angles from the 620 and 408 Mc/s observations. The first assumption that has been made in this calculation is that the position angle of the E vector of the polarized radiation varies as the square of the wavelength, so that the rotation measures calculated from the 620 and 408 Mc/s polarization angles may be used to extrapolate back to zero wavelength to obtain the intrinsic polarization angle; for example, a rotation measure of 1 indicates that the intrinsic angle lies 14° from the 620 Mc/s polarization angle. This seems a reasonable assumption, since Gardner and Whiteoak (1963) have found that the polarized radiation from most radio sources obeys the λ^2 law. Also, Komesaroff (personal communication) has shown theoretically that the λ^2 law should hold approximately until the wavelength has increased to the point at which the degree of polarization has fallen to a small fraction of its "zero-wavelength" value. From Paper I, it appears that the degree of polarization at 408 Mc/s is still quite high (about 30%), so that the λ^2 law should still hold.

A second assumption that has been made is that the difference in aerial beamwidths at 620 and 408 Mc/s does not appreciably affect the result. Ideally, the aerial beams should be identical at the two frequencies so that the same volume of space is observed. However, it is seen from Figure 1 that, in most regions, the E vectors at both frequencies are remarkably well ordered over much larger areas

---

Fig. 2.—Positions listed in Table 3 (indicated by the dots). The number to the right of a dot gives the rotation measure (rad/m^2) to the nearest integer, while the number to the left gives the ratio of the polarization temperatures at 408 and 620 Mc/s, to the nearest integer. The rotation measures of the discrete radio sources that have been measured by Gardner and Davies (1966) are plotted inside the circles shown.

than the aerial beams, and therefore the difference in the areas covered by the aerial beams should not introduce any serious error.

Table 4

RESULTS OF 1410 MC/S POLARIZATION OBSERVATIONS

l^{II} (deg)	b^{II} (deg)	T_b^p (°K)	θ_{gal}	θ_{gal} (intr.)
347	+64	0·4	6	2
350	+66	0·4	14	12
354	+67	0·6	179	2
334	+45	0·4	178	10
334	+38	0·4	158	178
336	+40	0·5	161	171
337	+42	0·4	169	16
340	+41	0·7	167	11
341	+42	0·6	171	18
343	+41	0·6	2	45
345	+43	0·5	7	170
347	+42	0·5	14	4
349	+43	0·4	10	165
351	+42	0·4	7	19
326	−4	0·4	170	160
328	−6	0·6	170	162
18	−5	0·4	148	150
20	−4	0·4	130	118
342	−32	0·6	154	166
344	−32	0·5	30	172
348	−28	0·5	176	141
350	−26	0·4	22	5
354	−23	0·6	29	3
3	−22	0·5	1	165
322	−36	0·4	123	135
322	−46	0·5	11	132
324	−45	0·4	27	18
334	−45	0·4	13	—
336	−46	0·4	10	—
338	−49	0·4	0	22
339	−47	0·4	14	—
340	−44	0·5	29	106
352	−44	0·4	8	108
354	−42	0·4	13	173
357	−40	0·4	18	170
2	−39	0·4	158	158
151	−51	0·4	117	113

The deduced intrinsic polarization angles are shown in Figure 3. The dotted coordinate lines in the diagram are sections of the great circle passing through the

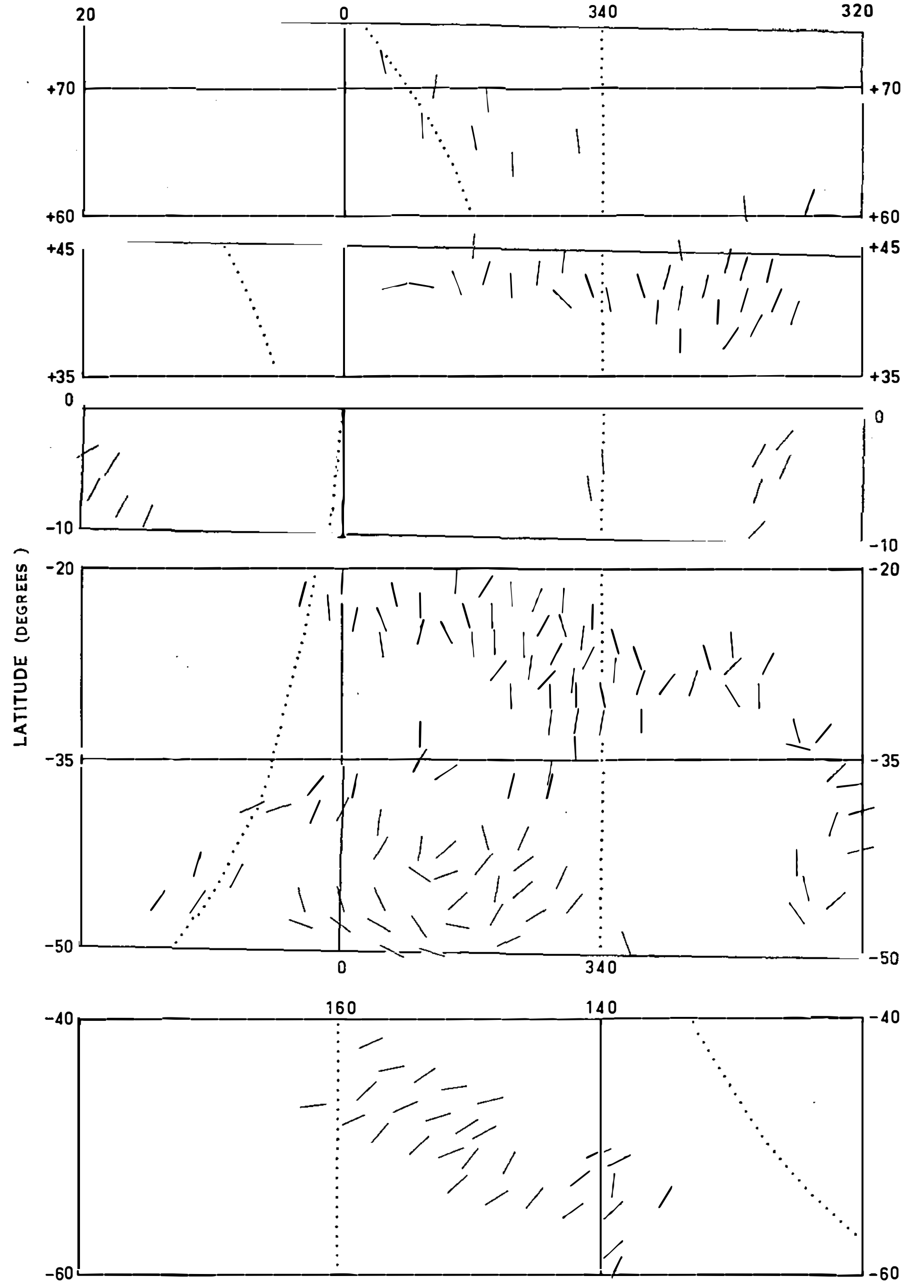

Fig. 3.—Intrinsic polarization angles calculated from the 620 and 408 Mc/s observations. The dotted coordinate lines are sections of the great circle passing through the galactic poles and intersecting the plane at $l^{\mathrm{II}} = 340°$ and 160°. Sections of a small circle, parallel to this great circle and lying 10° from the midline of the band containing the 408 Mc/s polarization, are also dotted in. In the north polar zone at the top of the diagram, the curved dotted line is a small circle parallel to *the* great circle and which intersects the plane at $l^{\mathrm{II}} = 345°$.

galactic poles and intersecting the plane at $l^{\mathrm{II}} = 340°$ and 160°. Sections of a small circle parallel to this great circle and intersecting the plane at $l^{\mathrm{II}} = 0°$ and 140° are also dotted in. This small circle is 10° from the midline of the band containing the 408 Mc/s polarization. This midline is the small circle that intersects the plane at $l^{\mathrm{II}} = 350°$ and 150° (Paper I). In the north polar zone at the top of Figure 3, the curved dotted line is a small circle parallel to *the* great circle and which intersects the plane at $l^{\mathrm{II}} = 345°$. Using the dotted lines as guides, it is seen that the intrinsic polarization angles lie approximately along the band with the exception of the region at the bottom of the figure (see part (*d*) of this section). This new evidence gives strong support to the model proposed in Paper I.

Similar results are found in other parts of the band, which were studied by the Dutch investigators (Berkhuijsen and Brouw 1963, 408 Mc/s; Muller *et al.* 1963 and Berkhuijsen *et al.* 1964, 610 Mc/s). They found a region of small rotation measure extending from $l^{\mathrm{II}} = 130°$, $b^{\mathrm{II}} = -40°$ up to $l^{\mathrm{II}} = 140°$, $b^{\mathrm{II}} = +10°$. The intrinsic polarization angles in this band are almost parallel to *the* great circle. Also, the intrinsic polarization angles were calculated from their results for the north galactic polar regions and were found to lie approximately parallel to the line joining $l^{\mathrm{II}} = 340°$ and $l^{\mathrm{II}} = 160°$. These results give additional support to the proposed model.

Table 4 gives the polarization angles at 1410 Mc/s for 37 of the positions of Table 3. At this frequency, these angles should lie quite close to the intrinsic angles since the rotation measures are small. It is found that the polarization angles have a mean deviation of about 20° from the intrinsic angles calculated from the 620 and 408 Mc/s observations. However, this comparison has not much significance because the probable error of the 1410 Mc/s polarization angles is about 15° (owing to the low values of $T_{\mathrm{b}}^{\mathrm{p}}$ at this frequency) and because the aerial beam at 1410 Mc/s covers less than one-fifth the area of the 620 Mc/s beam.

(*b*) *Magnetic Field Directions*

The intrinsic polarization angle is related to the transverse magnetic field component at emission, whilst the rotation measure depends on the longitudinal component of the magnetic field along the line-of-sight. Interpretation of the rotation measures is complicated in practice, since the Faraday rotation can take place throughout the emission region as well as in the intervening medium.

A feature of Figure 2 is that the sense of the rotation remains the same over quite large areas. This indicates that the magnetic field has a uniform direction in this region. Ideally, on the basis of the proposed model, there should be a systematic trend in the rotation measure across the band. The rotation measures should be of opposite sign at either side of the band, with a region of zero rotation measure at the centre where the line-of-sight is normal to the magnetic field. The rotation measures should increase in magnitude as the edges of the band are approached. Berkhuijsen *et al.* (1964) found such a systematic trend in the strongly polarized region centred on $l^{\mathrm{II}} = 140°$, $b^{\mathrm{II}} = +10°$. From the sense of the rotation measure on either side of the centre, they determined that the magnetic field in this region was directed towards $l^{\mathrm{II}} = 70°$.

There is a suggestion of a systematic trend in the rotation measures of several of the regions shown in Figure 2, although more observations are needed to confirm this. For example, the region centred on $l^{\mathrm{II}} = 345°$, $b^{\mathrm{II}} = -27°$ has predominantly negative R.M. at high longitudes, with an area of zero R.M. near the centre. However, there seems to be a mixture of positive and negative R.M. on the low longitude side. Similarly, the region at $b^{\mathrm{II}} = +42°$ in Figure 2 has negative R.M. at high longitudes, and towards low longitudes has a region of zero R.M. with several positive R.M. points near the edge. The region centred on $l^{\mathrm{II}} = 353°$, $b^{\mathrm{II}} = -47°$ also has negative R.M. at high longitudes with positive R.M. at low longitudes. These results suggest that the magnetic field is directed towards $l^{\mathrm{II}} = 70°$, which is in the same direction found by Berkhuijsen *et al.* for the region at $l^{\mathrm{II}} = 140°$, $b^{\mathrm{II}} = +10°$.

There are some anomalies. For example, there are some positive R.M. points on the high longitude side of the band in the region of $l^{\mathrm{II}} = 8°$, $b^{\mathrm{II}} = -42°$. The positions at latitudes greater than $+60°$ in Figure 2 have positive R.M. Berkhuijsen *et al.* also found that the rotation measures in this north polar zone were mostly positive, indicating a magnetic field component towards the observer. It is interesting to note that Gardner and Davies (1966) also concluded from a study of the polarization of extragalactic radio sources that the magnetic field has an inward direction at high latitudes.

The rotation measures of the extragalactic radio sources that have been measured by Gardner and Davies (1966) have been plotted inside the circles in Figure 2. Gardner and Davies place an upper limit of 5 on the rotation measure due to Faraday rotation in the source itself, and the remainder occurs in the ionized hydrogen and the magnetic fields in the local spiral arm. It is seen that the rotation measures due to the local arm are in general greater than the rotation measures of the polarized regions. This suggests that the polarized emission comes from close to the Sun, and arguments given in Paper I indicate a distance of 100–200 pc.

(*c*) *Depolarization*

The 408 and 620 Mc/s polarization temperature ratios, which give a measure of the apparent spectral index of the polarized radio emission, are given at the left-hand side of the position dots in Figure 2. Only a rough estimate of the spectral index is possible because of the closeness of the two frequencies and the relatively large error in the measurement of the polarization temperatures (Section IV).

Depolarization processes reduce the 408 Mc/s temperature relative to the 620 Mc/s temperature, so that these ratios may not give the spectral index of the radiation at emission. Depolarization may occur if Faraday rotation takes place throughout the emission region or by differential Faraday rotation across the aerial beam.

The average ratio for the points in Figure 2 is only a little greater than 2, which indicates a flux-density spectral index of zero. This is "flatter" than the value of $-0 \cdot 6$ found for unpolarized galactic radio emission, so that depolarization is probably taking place. However, the expected correlation between the spectral index and the rotation measure is not found. This may be masked if Faraday rotation is also taking place uniformly across the whole aerial beam. The positions lying in the region at the bottom in Figure 2 have a "steeper" spectral index than the positions in the other regions. This will be discussed in (*d*) below.

(d) *The Cetus Arc*

In the region shown in the bottom diagram of Figure 3, the intrinsic polarization angles do not line up with the dotted lines but lie at about 60° to them. This region forms part of the Cetus Arc which Large, Quigley, and Haslam (1962) suggested is a supernova remnant.

The 237 Mc/s continuum map of this area given by Large, Quigley, and Haslam is reproduced in Figure 4, and on this map the areas of strong 408 Mc/s polarization are indicated by shading. It is seen that the polarization coincides with a section

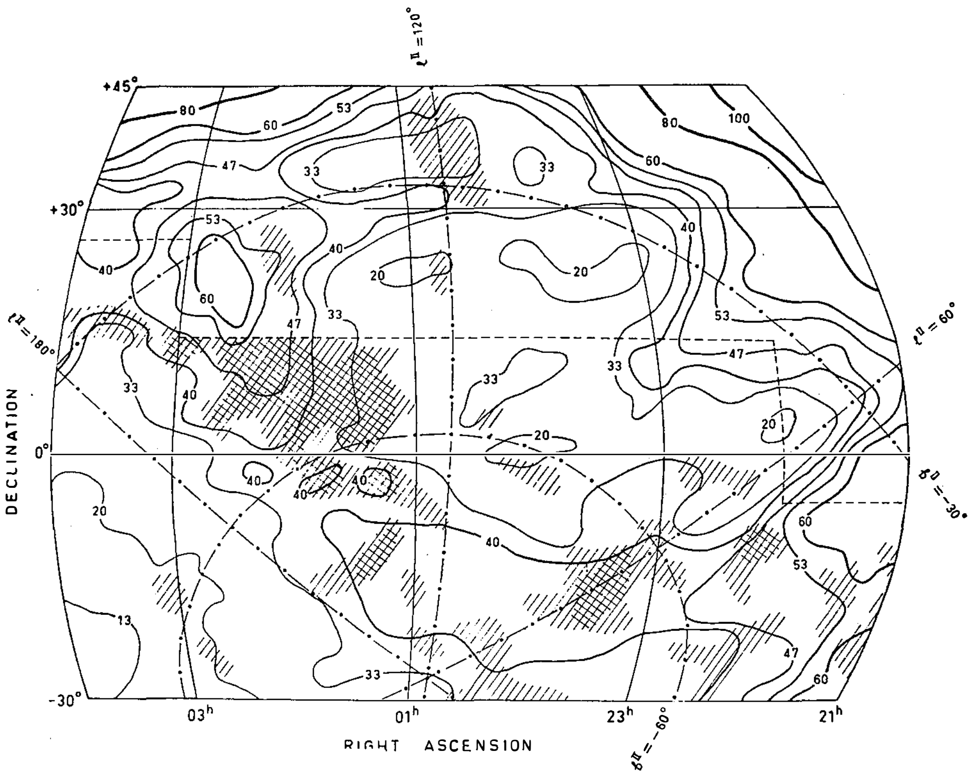

Fig. 4.—The region of the Cetus Arc. The 408 Mc/s polarized region contained within the no. 3 contour of polarization brightness temperature as shown in Figure 3, Paper I, is shaded, and the region within the no. 4 contour is cross-hatched onto the 237 Mc/s continuum isophotes of Large, Quigley, and Haslam (1962).

of the ridge of emission of the Cetus Arc. It is interesting to note that the direction of the magnetic field, which from synchrotron radiation theory is perpendicular to the intrinsic polarization angle, lies along the ridge line.

The rotation measures of the positions at low longitudes in the Cetus Arc (Fig. 2) are mostly zero. However, at $l^{\mathrm{II}} = 142°$, the rotation measure suddenly increases with a positive sense. It is seen from Figure 4 that the points at high longitudes lie on a more intense part of the ridge. It may be argued that the increase in rotation measure is due to an increase in Faraday rotation throughout the emission region. However, in Section V of Paper I a comparison of the high- and low-frequency continuum surveys revealed the presence of an extended HII region centred on $l^{\mathrm{II}} = 150°$, $b^{\mathrm{II}} = -30°$. Since the positions with high rotation measure lie near this region, it seems more reasonable to assume that the Faraday rotation occurs in the outer regions of this ionized gas cloud.

It has been noticed that the positions in the Cetus Arc in Figure 2 have "steeper" spectral indices than the positions in the other regions. Berkhuijsen *et al.* (1964) and Gardner (1964) have also commented on the steep spectral indices in this region. This explains why all but one of the points in Figure 2 have polarization temperatures less than 0·3°K at 1410 Mc/s. However, it is surprising that no polarization was found at 152 Mc/s considering the steep spectral index and the fact that polarization was found at this frequency in the other regions.* If the Cetus Arc is part of a supernova remnant, it may have a different electron energy spectrum from the other "synchrotron" regions, which are suggested in Paper I to be structural features of the spiral arm.

VI. Conclusion

Observations at 620 and 408 Mc/s have been used to determine the intrinsic polarization of galactic radio emission in the strong extended regions of the band of polarization discovered at 408 Mc/s (Paper I). Many of the intrinsic polarization angles lie nearly parallel to the approximate midline of the band, i.e. the great circle passing through the galactic poles and intersecting the plane at $l^{\mathrm{II}} = 340°$ and 160°. This new observational evidence supports the explanation proposed in Paper I for the existence of the band, namely, that the emission is synchrotron radiation from regions in the local spiral arm that are pervaded by a fairly uniform magnetic field parallel to the line joining $l^{\mathrm{II}} = 70°$ and $l^{\mathrm{II}} = 250°$. Analysis of the rotation measures of these regions suggests that the magnetic field is directed towards $l^{\mathrm{II}} = 70°$.

VII. Acknowledgment

The authors thank Dr. J. A. Roberts for his critical reading of the manuscript and for his many helpful comments.

VIII. References

Berkhuijsen, E. M., and Brouw, W. N. (1963).—*Bull. Astr. Insts Neth.* **17**: 185.

Berkhuijsen, E. M., Brouw, W. N., Muller, C. A., and Tinbergen, J. (1964).—*Bull. Astr. Insts Neth.* **17**: 465.

Cooper, B. F. C., and Price, R. M. (1962).—*Nature* **195**: 1084.

Gardner, F. F. (1964).—Symp. IAU–URSI No. 20 (Canberra 1963). p. 143.

Gardner, F. F., and Davies, R. D. (1966).—*Aust. J. Phys.* **19**: 129–39.

Gardner, F. F., and Whiteoak, J. B. (1963).—*Nature* **197**: 1162.

Kellermann, K. I. (1964).—*Publs Owens Valley Radio Obs.* **1**: 1.

Large, M. I., Quigley, M. J. S., and Haslam, C. G. T. (1962).—*Mon. Not. R. Astr. Soc.* **124**: 405.

Mathewson, D. S., and Milne, D. K. (1965).—*Aust. J. Phys.* **18**: 635.

Muller, C. A., Berkhuijsen, E. M., Brouw, W. N., and Tinbergen, J. (1963).—*Nature* **200**: 155.

Seeger, C. L., Westerhout, G., and van de Hulst, H. C. (1956).—*Bull. Astr. Insts Neth.* **13**: 89.

Wielebinski, R., and Yates, K. W. (1965).—*Nature* **205**: 581.

* At 152 Mc/s, polarization temperatures of about 15°K were found at the positions whose right ascensions and declinations are $19^{\mathrm{h}}12^{\mathrm{m}}$, $-50°$; $19^{\mathrm{h}}12^{\mathrm{m}}$, $-48°$; $14^{\mathrm{h}}32^{\mathrm{m}}$, $-16°$; and $14^{\mathrm{h}}40^{\mathrm{m}}$, $-14°$.